

# A reverse pendulum bath cryostat design suitable for low temperature scanning probe microscopy

M Heyde, G Thielsch, H-P Rust and H-J Freund

Fritz-Haber-Institut der Max-Planck-Gesellschaft, Faradayweg 4-6, D-14195 Berlin, Germany

E-mail: heyde@fhi-berlin.mpg.de

Received 6 July 2004, in final form 15 December 2004

Published 11 February 2005

Online at [stacks.iop.org/MST/16/859](http://stacks.iop.org/MST/16/859)

## Abstract

A new low temperature, ultrahigh vacuum cryostat design has been developed for atomic force and scanning tunnelling microscopy measurements. A microscope can be operated at 5 K in ultrahigh vacuum. The microscope body is thermally connected to a reverse pendulum and completely surrounded by a radiation shield. The design allows *in situ* dosing and irradiation of the sample as well as for easy access of tip and sample. The temperature performance and the vibrational properties of the reverse pendulum design are demonstrated in detail. A brief overview of low temperature instrumentation in scanning probe microscopy is given.

**Keywords:** cryogenics instrumentation, microscopy, atomic force instrumentation, scanning tunnelling instrumentation

## 1. Introduction

Since the invention of the scanning tunnelling microscope (STM) and the atomic force microscope (AFM), it has been desirable to perform experiments at temperatures other than ambient. Imaging at cryogenic temperatures opens up a wide range of experiments, where atomic diffusion processes and thermal fluctuations are reduced [1]. Atoms on conducting substrates have been imaged by STM and on insulating substrates by AFM. Low temperature instrumentation allows one to move atoms on a surface [2], to break [3] and make molecular bonds [4], and to design new structures at the atomic scale. Interesting surface and bulk properties have been investigated, including the observation of spin and Landau levels in semiconductors [5], the investigation of lifetime broadening effects of particular electronic states on the nanometre scale [6], the visualization of electronic wavefunctions in real space [7] and the detection [8] and localization of vibrational levels within particular molecules via inelastic tunnelling. Many physical effects guided by electronic correlations such as superconductivity, the Kondo effect and many of the electron phases found in semiconductors are restricted to low temperatures. Additionally and rather importantly the stability of the experimental set-up, in which

the whole microscope body is kept at a constant low temperature, is widely improved through reduction in piezo hysteresis and creep, reduced thermal drift, lower noise levels and enhanced stability of tip and sample. The attempt to combine good thermal contact to a liquid helium reservoir with vibration isolation of the microscope is the difficulty in designing a cryogenic STM or AFM. The early designs of low temperature STMs involved immersing the microscope directly [9, 10] in liquid nitrogen or liquid helium. In numerous papers, various designs of STMs and AFMs, based on the use of continuous flow and bath cryostats, have been reported [11–25]. Below, a selected number of low temperature instrumentations in use will be reviewed. In this paper, we present a new concept of a low temperature bath cryostat set-up suitable for STM and AFM experiments, and include a description of the cryogenic performance and the vibrational properties of the system.

## 2. Overview of cryostats

### 2.1. Bath cryostats

The design of the helium-cooled STM shown in figure 1 was invented by Eigler and co-workers [26]. A pendulum

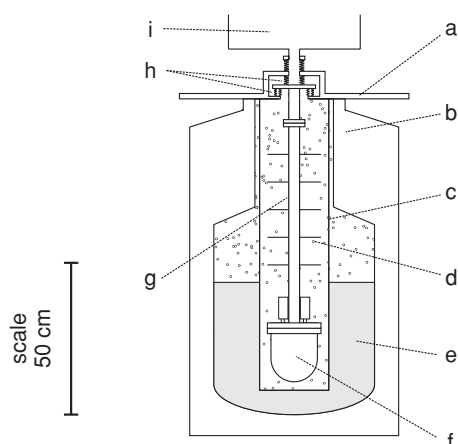


**Figure 1.** Schematic of an Eigler-style bath cryostat. Support plate (a), Dewar (b), exchange gas canister (c), radiation shields (d), liquid helium (e), microscope (f), pendulum (g), vibrational isolation (h), ultrahigh vacuum chamber (i).

is used to provide mechanical vibrational insulation. At its end, the STM head is in an ultrahigh vacuum environment while the upper end is suspended from a set of stainless steel bellows, giving the STM head the freedom to swing in all directions at a frequency of about 1 Hz. The pendulum is placed inside an exchange gas canister, which in turn is inserted into a liquid helium Dewar<sup>1</sup>. Radiation shields are mounted along the length of the pendulum. The volume of the canister is evacuated, and then backfilled with helium gas (1–10 mbar) for thermal coupling and acoustic insulation of the microscope. The typical consumption rate of liquid helium is  $0.5 \text{ l h}^{-1}$  at a temperature of 4 K [27]. The first manipulation of single atoms and molecules was performed with such a design [2, 28]. Those experiments, and the visualization of the standing electron waves of the surface state on Cu(111) [7, 29], are just a few examples of the spectacular results obtained with such instrumentation. Also, diffusion experiments of carbon monoxide molecules on Cu(110) in the temperature range between 42 and 53 K [30] as well as the procedure for operating such a bath cryostat design at variable temperatures have been presented [31]. Recently, such a cryostat design has been used to record simultaneous STM and AFM measurements [32].

Another design has been realized using on top bath cryostats, which are manufactured as a standard cryostat for the low temperature range. On top bath cryostats (figure 2) are available with various neck diameters and capacities, consisting of a vacuum chamber, liquid helium tank, liquid nitrogen tank and radiation shields. The liquid nitrogen shield and the liquid nitrogen vessel are built around the liquid helium vessel, so that the heat radiation from the room temperature is shielded. In such a set-up, the whole microscope is surrounded by two concentric radiation shields (figure 2). The inner one at 4 K is directly connected to the liquid helium tank and the outer one at 77 K is connected to the liquid nitrogen tank. Typical consumption rates are less than  $0.1 \text{ l h}^{-1}$  for liquid helium and  $0.4 \text{ l h}^{-1}$  for liquid nitrogen<sup>2</sup>. The boiling of liquid nitrogen might cause some significant

<sup>1</sup> Precision Cryogenic Systems, Inc., 7804 Rockville Road, Indianapolis, IN 46214, USA.

<sup>2</sup> Cryovac GmbH and Co. KG, Heuserweg 14, D-53842 Troisdorf, Germany.

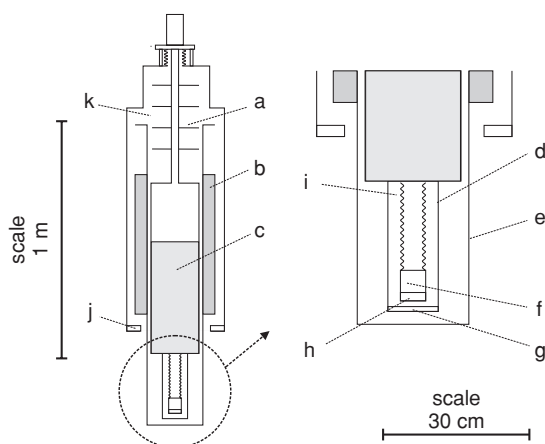


**Figure 2.** Schematic of an on top bath cryostat. Radiation shields (a), liquid nitrogen tank (b), liquid helium tank (c), helium cooled shield (d), nitrogen cooled shield (e), microscope body (f), cool down cavity (g), eddy current damping (h), springs and electrical wires (i), cryostat support flange (j), ultrahigh vacuum (k).

mechanical vibrations, which can be minimized by lowering the pressure in the liquid nitrogen tank under the triple point of nitrogen. In the operating position, the microscope hangs from springs which results in good mechanical vibration isolation but weak thermal contact to the liquid helium reservoir. On the other hand, the microscope is surrounded by a radiation shield so that no thermal radiation falls on the microscope, which means that the microscope is almost thermally isolated. The electrical connections to the microscope are thermally anchored at the bottom of the liquid helium tank. The cooling down process of the microscope is performed simply by mechanically clamping the microscope body into the inner radiation shield. The microscope is capable of operating in a temperature range of 5 K to RT. Such a set-up [20] has been used for atomic manipulation, in which all steps of a chemical reaction have been induced with the STM tip [33].

## 2.2. Flow cryostats

A continuous flow cryostat set-up [18, 34–36] is not limited to a fixed cryogenic temperature and allows for microscope operation at different temperatures. The experimental set-up shown in figure 3 illustrates a flow cryostat design<sup>3</sup> with two radiation shields [36], which can be operated from 8 to 350 K in ultrahigh vacuum. The cryogen usage is approximately  $1.3 \text{ l h}^{-1}$  at 8 K. The cryostat is supplied by a flexible transfer line connected to the Dewar. The transfer line contains a vacuum jacket and a cooled shield to keep the thermal losses low (figure 3(a)). The inner radiation shield (figure 3(n)) is bolted directly to the end of the cold tip of the cryostat in ultrahigh vacuum. The cooling support temperature is regulated by adjusting the cryogen flow rate with a needle valve and with the use of a heater wrapped around the cooling support. The heater is operated and optimized with a temperature controlled feedback loop. The outer copper radiation shield (figure 3(o)) is cooled by the helium exhaust gas from the cooling support. Similar to the previously described on top bath cryostat set-up, the

<sup>3</sup> APD Cryogenics LT-3B, 1833 Vultee Street, Allentown, PA 18103, USA.

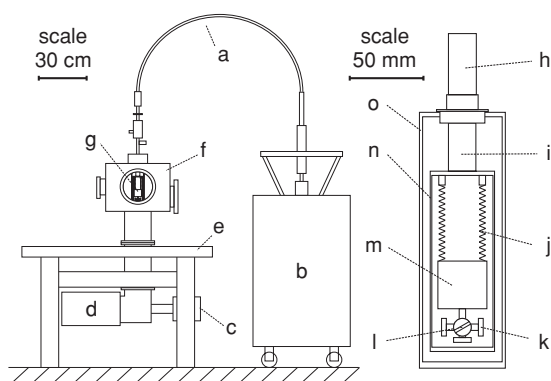


**Figure 3.** Schematic of a continuous flow cryostat design [36]. Liquid helium transfer line (a), liquid helium Dewar (b), turbo pump (c), ion getter pump (d), air floated table (e), ultrahigh vacuum chamber (f), microscope (g), continuous flow liquid helium/nitrogen cryostat (h), cooling support (i), springs and electrical wires (j), eddy-current damping (k), clamping screw (l), microscope (m), inner shield (n), outer shield (o).

microscope is suspended by springs from the cooling support for vibrational decoupling from the flow cryostat and external noise. The inner radiation shield is equipped with a screw used to clamp the microscope assembly against the back wall of the shield for rapid cool down. Flow cryostat set-ups have been used for experiments on single atoms and molecules, which have been conducted to study adsorption, electronic and vibrational excitations of adsorbates and the coupling of electrons to nuclear motion [37]. Studies of single molecule dissociation [38, 39] and rotation [8] were likewise used to determine potential energy barriers, vibrational relaxation rates and electron–vibration coupling constants.

### 3. Reverse pendulum design

A new low temperature, ultrahigh vacuum cryostat design has been developed that is suitable for STM and AFM measurements. The experimental set-up allows for a huge variety of *in situ* investigations, due to the great accessibility of the cooling support and accordingly the microscope body. The design is ideal for *in situ* deposition of gases and metals onto a cold sample. STM-induced photon emission experiments as well as fibre interferometry AFM set-ups could also be housed. The reverse pendulum set-up is built into a bath cryostat (see footnote 1) and an ultrahigh vacuum system that comprises two vacuum chambers (figure 4). One chamber is used for sample preparation, which also serves as a transfer chamber, and the other houses the reverse pendulum/microscope assembly and other surface analysis techniques, such as LEED and Auger electron spectroscopy. The entire set-up is supported by an active isolation system MOD-4,<sup>4</sup> which consists of four isolation elements placed under the load of the ultrahigh vacuum chamber and the cryostat. The active vibration isolation has excellent low frequency damping in the critical range of 0.7 and 5 Hz. A transmission factor of 0.1 is already achieved at a frequency of 5 Hz, and a factor of 0.02 at 30 Hz. A wooden frame (figure 4(f)) placed on top of the isolation elements supports the load of the ultrahigh

<sup>4</sup> Halcyonics GmbH, Anna Vanenhoeck-Ring 5, D-37081 Göttingen, Germany.

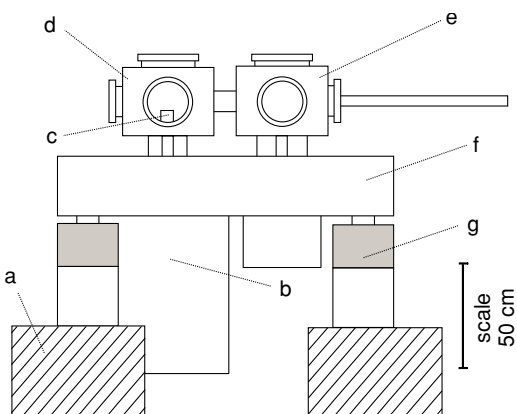


**Figure 4.** Schematics of the entire two-chamber ultrahigh vacuum and reverse pendulum bath cryostat system. Separate foundation with pit (a), bath cryostat (b), shielded microscope support (c), main chamber (d), preparation chamber (e), wooden frame (f), active isolation elements (g).

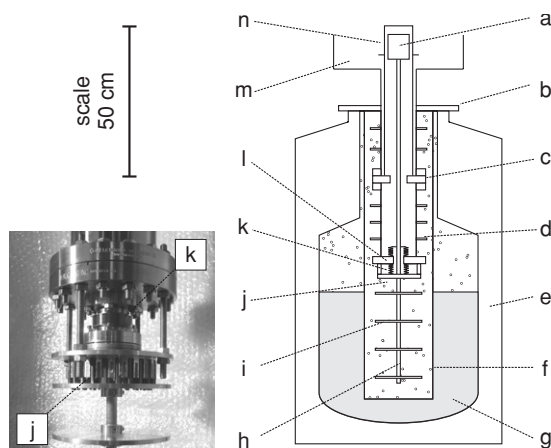


**Figure 5.** Schematics of the new bath cryostat design. Microscope support (a), cryostat support at room temperature (b), support of the inner radiation shield (c), outer radiation shields (d), Dewar (e), exchange gas canister (f), liquid helium (g), copper pendulum (h), lower shields for thermal coupling (i), eddy current damping (j), bellows (k), pendulum support (l), ultrahigh vacuum chamber (m), inner radiation shield (n).

vacuum system. The hole system is additionally housed in an acoustic hood<sup>5</sup> for decoupling external acoustic noise from the experimental set-up. The described vibration isolation is commonly used to isolate an experiment from the lab's noisy environment. Unfortunately, for low temperature experiments, it is often the cryogen itself, e.g. the boiling liquid nitrogen and liquid helium and the pings of contracting materials, which produces troublesome vibrations. In such cases, isolation of the microscope from the noisy environment, namely the bath cryostat, is often difficult and at odds with the strong contact required for thermal reasons.

The reverse pendulum is the main design feature for providing internal mechanical vibrational insulation and good thermal coupling to the liquid helium reservoir. A schematic view of the cryostat set-up and a picture of the internal damping system are given in figure 5. The pendulum is made of an

<sup>5</sup> Industrial Acoustics Company GmbH, Sohlweg 17, D-41372 Niederkrüchen, Germany.

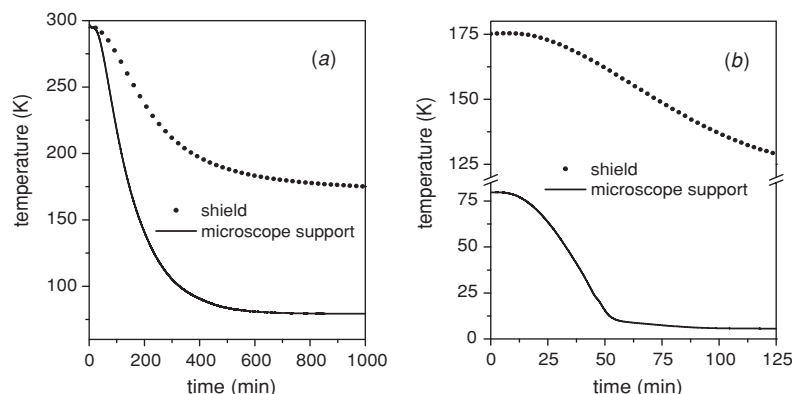


**Figure 6.** Temperatures measured at the microscope support and shield versus time of the cool-down process with liquid nitrogen (a) and liquid helium (b).

oxygen free highly conductive copper rod. At its top, the microscope head is in an ultrahigh vacuum environment while the lower part is suspended from a set of stainless steel bellows in combination with an eddy current damping system. A picture of the eddy current damper is given in figure 5(j), where magnets are interdigitated with copper plates. The reverse pendulum and the ultrahigh vacuum support are placed inside an exchange gas canister (figure 5(f)), which in turn is inserted into a liquid helium Dewar (see footnote 1). Shields are mounted along the length of the lower part of the pendulum and around the ultrahigh vacuum support (figures 5(d), (i)). An inner radiation shield (figure 5(n)) is mounted at the support (figure 5(c)) inside the ultrahigh vacuum chamber to reduce thermal radiation. The exchange gas canister is used to provide isolation of the pendulum from vibrations caused by the cryogen. The interior of the exchange gas canister can be filled with helium gas to regulate the thermal coupling of the bath to the pendulum. In order to cool the microscope, the volume of the canister is evacuated, and then backfilled with helium gas. This exchange gas is cooled by interaction with the walls of the gas canister in contact with the liquid cryogen. A helium gas pressure of about 10 mbar is needed to operate the microscope body at a temperature of 5 K.

### 3.1. Cryogenic properties

Microprocessor-based temperature instruments<sup>6</sup> have been used to operate the silicon diode temperature sensors<sup>7</sup> to furnish accurate temperature measurements. One silicon diode has been mounted onto the radiation shield (figure 5(n)) and the other has been connected to the microscope support (figure 5(a)). Thermal anchoring of the connecting wires was necessary to assure that the sensor and the leads are at the same temperature as the sample. The silicon diode has been calibrated at 4.2 K. It has a temperature range from 1.4 K to 475 K and a low temperature accuracy of  $\pm 0.5$  K. Figure 6 shows the cooling performance for liquid nitrogen and liquid helium. The cool down process with liquid nitrogen needs 10 h until a stable temperature at the microscope support of 79 K is achieved. After the exchange for liquid helium

<sup>6</sup> MD 1901, Scientific Instruments, Inc., 4400 W Tiffany Drive, West Palm Beach, FL 33407, USA.

<sup>7</sup> DT-470-SD-12, Lake Shore Cryotronics, Inc., 575 McCorkle Blvd, Westerville, OH 43082, USA.

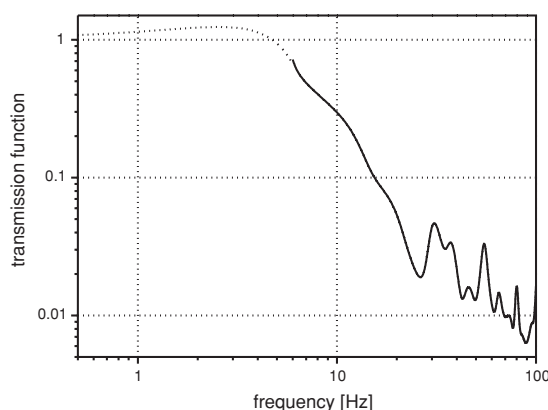


**Figure 7.** Experimental transfer function of the low temperature magnetic damped reverse pendulum stage measured with an accelerometer (see footnote 8) from 5 Hz up to 100 Hz. The transfer function is defined as the ratio of the amplitude of vibration detected on the reverse pendulum and on the ultrahigh vacuum chamber. The cut-off takes place for frequencies higher than 5 Hz and transmission by a factor of 0.1 is already reached at a frequency of 15 Hz and falls to 0.01 at 70 Hz. These filtering characteristics are similar to commonly used room temperature Viton stacks.

as coolant, the microscope support reaches a minimum temperature of 5 K within 1 h. The temperature stability of the microscope support is better than 0.1 K, which is the resolution of our temperature sensor. The helium consumption is around  $0.6 \text{ l h}^{-1}$  to maintain the temperature at 5 K. The consumption rate of liquid helium is slightly higher compared to the previously described bath cryostat set-ups (figures 1 and 2), but still significantly lower than the consumption of the flow cryostat designs. By optimizing the position of the radiation shields as well as by further adjusting the pressure in the gas exchange canister a lower consumption rate of liquid helium might be obtained.

### 3.2. Vibrational isolation performance

To use the reverse pendulum design for STM and AFM experiments, special attention has to be paid to mechanical stability of the microscope itself. Microscope bodies for low temperature STM and AFM are usually designed to have a very high resonance frequency, thus decreasing the sensitivity to

external vibrations. High resonance frequencies are obtained by constructing the microscope body rigid, lightweight and as compact as possible [23]. The motion of the reverse pendulum has been sensed by using a servo accelerometer sensor and a signal amplifier<sup>8</sup>. The data acquisition has been realized with a fast Fourier transform analyser<sup>9</sup> and a serial data recording interface to measure the amplitude spectrum of the pendulum. The measurements have been performed at room temperature. The resonance frequency of the pendulum is in the horizontal direction 0.6 Hz and in the vertical direction 3.4 Hz. To characterize the efficiency of our magnetic damped reverse pendulum, its complete transfer function for frequencies higher than 5 Hz has been measured. The experimental transfer function is shown in figure 7 and has been obtained by vibrating the damping set-up with a commercial loudspeaker while measuring the amplitude of the vibration on the ultrahigh vacuum chamber and on the reverse pendulum. It can be clearly seen that the pendulum design acts as a low pass filter and it is very effective.

## Acknowledgments

MH thanks U D Schwarz for fruitful discussions on low temperature scanning probe microscopy designs. HPR would also like to acknowledge very helpful discussions with J I Pascual and H Conrad. Financial support from the German Science Foundation within the SFB 290 TPA9 (MH) is also gratefully acknowledged.

## References

- [1] Bhushan B 2004 *Handbook of Nanotechnology* (Berlin: Springer)
- [2] Eigler D M and Schweizer E K 1990 Positioning single atoms with a scanning tunneling microscope *Nature* **344** 524–6
- [3] Dujardin G, Walkup R E and Avouris Ph 1992 Dissociation of individual molecules with electrons from the tip of a scanning tunneling microscope *Science* **255** 1232–5
- [4] Lee H J and Ho W 1999 Single-bond formation and characterization with a scanning tunneling microscope *Science* **286** 1719–22
- [5] Morgenstern M, Haude D, Gudmundsson V, Wittneven C, Dombrowski R and Wiesendanger R 2000 Origin of Landau oscillations observed in scanning tunneling spectroscopy on n-InAs(110) *Phys. Rev. B* **62** 7257–63
- [6] Kliewer J, Berndt R, Chulkov E V, Silkin V M, Echenique P M and Crampin S 2000 Dimensionality effects in the lifetime of surface states *Science* **288** 1399–402
- [7] Crommie M F, Lutz C P and Eigler D M 1993 Imaging standing waves in a 2-dimensional electron-gas *Nature* **363** 524–7
- [8] Stipe B C, Rezaei M A and Ho W 1998 Inducing and viewing the rotational motion of a single molecule *Science* **279** 1907–9
- [9] Smith D P E and Binnig G 1986 Ultrasmall scanning tunneling microscope for use in a liquid helium storage dewar *Rev. Sci. Instrum.* **57** 2630–1
- [10] Elrod S A, de Lozanne A L and Quate C F 1984 Low-temperature vacuum tunneling microscopy *Appl. Phys. Lett.* **45** 1240–2
- [11] Lang C A, Dovek M M and Quate C F 1989 Low-temperature ultrahigh-vacuum scanning tunneling microscope *Rev. Sci. Instrum.* **60** 3109–12
- [12] Giessibl F J, Gerber Ch and Binnig G 1991 A low-temperature atomic force/scanning tunneling microscope for ultrahigh vacuum *J. Vac. Sci. Technol. B* **9** 984–8
- [13] Wolkow R A 1992 A variable temperature scanning tunneling microscope for use in ultrahigh vacuum *Rev. Sci. Instrum.* **63** 4049–52
- [14] Roder H, Brune H, Bucher J P and Kern K 1993 Changing morphology of metallic monolayers via temperature-controlled heteroepitaxial growth *Surf. Sci.* **298** 121–6
- [15] Reihl B, Gimzewski J K, Schlittler R, Tschudy M, Brendt R, Gaisch R and Schneider W D 1994 Low-temperature scanning tunneling microscopy *Physica B* **197** 64–71
- [16] Schulz R R and Rossel C 1994 Beetle-like scanning tunneling microscope for ultrahigh vacuum and low-temperature applications *Rev. Sci. Instrum.* **65** 1918–22
- [17] Wildöer J W G, van Roy A J A, van Kempen H and Harmans C J P M 1994 Low-temperature scanning tunneling microscope for use on artificially fabricated nanostructures *Rev. Sci. Instrum.* **65** 2849–52
- [18] Horch S, Zeppenfeld P, David R and Comsa G 1994 An ultrahigh vacuum scanning tunneling microscope for use at variable temperature from 10 to 400 K *Rev. Sci. Instrum.* **65** 3204–10
- [19] Smith A R and Shih C K 1995 New variable low-temperature scanning tunneling microscope for use in ultrahigh vacuum *Rev. Sci. Instrum.* **66** 2499–503
- [20] Meyer G 1996 A simple low-temperature ultrahigh-vacuum scanning tunneling microscope capable of atomic manipulation *Rev. Sci. Instrum.* **67** 2960–5
- [21] Allers W, Schwarz A, Schwarz U D and Wiesendanger R 1998 A scanning force microscope with atomic resolution in ultrahigh vacuum and at low temperatures *Rev. Sci. Instrum.* **69** 221–5
- [22] Hug H J, Stiefel B, vanSchendel P J A, Moser A, Martin S and Güntherodt H-J 1999 A low temperature ultrahigh vacuum scanning force microscope *Rev. Sci. Instrum.* **70** 3625–40
- [23] Pan S H, Hudson E W and Davis J C 1999 3He refrigerator based very low temperature scanning tunneling *Rev. Sci. Instrum.* **70** 1459–63
- [24] Pietzsch O, Kubetzka A, Haude D, Bode M and Wiesendanger R 2000 A low-temperature ultrahigh vacuum scanning tunneling microscope with a split-coil magnet and a rotary motion stepper motor for high spatial resolution studies of surface magnetism *Rev. Sci. Instrum.* **71** 424–30
- [25] Petersen L, Schunack M, Schaefer B, Linderoth T R, Rasmussen P B, Sprunger P T, Laegsgaard E, Stensgaard I and Besenbacher F 2001 A fast-scanning, low- and variable-temperature scanning tunneling microscope *Rev. Sci. Instrum.* **72** 1438–44
- [26] Weiss P S and Eigler D M 1993 What is underneath? Moving atoms and molecules to find out *Nanosources and Manipulations of Atoms under High Fields and Temperatures: Applications (NATO ASI Series E vol 235)* ed V T Binh, N Garcia and K Dransfeld (New York: Plenum)
- [27] Rust H-P, Buisset J, Schweizer E K and Cramer L 1997 High precision mechanical approach mechanism for a low temperature scanning tunneling microscope *Rev. Sci. Instrum.* **68** 129–32
- [28] Stroschio J A and Eigler D M 1991 Atomic and molecular manipulation with the scanning tunneling microscope *Science* **254** 1319–26
- [29] Heller E J, Crommie M F, Lutz C P and Eigler D M 1994 Scattering and absorption of surface electron waves in quantum corrals *Nature* **369** 464–6

<sup>8</sup> Model 305T and Model 515T, Kistler Instrument Corp., 75 John Glenn Drive, Amherst, NY 14228, USA.

<sup>9</sup> SR770 Single Channel FFT Spectrum Analyzer, Stanford Research Systems, Inc., 1290-D Reamwood Avenue, Sunnyvale, CA 94089, USA.

- [30] Briner B G, Doering M, Rust H P and Bradshaw A M 1997 Microscopic molecular diffusion enhanced by adsorbate interactions *Science* **278** 257–60
- [31] Rust H-P, Doering M, Pascual J I, Pearl T P and Weiss P S 2001 Temperature control of a liquid helium cooled Eigler-style scanning tunneling microscope *Rev. Sci. Instrum.* **72** 4393–7
- [32] Heyde M, Kulawik M, Rust H-P and Freund H-J 2004 Double quartz tuning fork sensor for low temperature atomic force and scanning tunneling microscopy *Rev. Sci. Instrum.* **75** 2446–50
- [33] Hla S W, Bartels L, Meyer G and Rieder K-H 2000 Inducing all steps of a chemical reaction with the scanning tunneling microscope tip: towards single molecule engineering *Phys. Rev. Lett.* **85** 2777–80
- [34] Bott M, Michely T and Comsa G 1995 Design principles of a variable-temperature scanning tunneling microscope *Rev. Sci. Instrum.* **66** 4135–9
- [35] Behler S, Rose M K, Dunphy J C, Ogletree D F and Salmeron M 1997 Scanning tunneling microscope with continuous flow cryostat sample cooling *Rev. Sci. Instrum.* **68** 2479–85
- [36] Stipe B C, Rezaei M A and Ho W 1999 A variable-temperature scanning tunneling microscope capable of single-molecule vibrational spectroscopy *Rev. Sci. Instrum.* **70** 137–43
- [37] Mitsui T, Rose M K, Fomin E, Ogletree D F and Salmeron M 2002 Water diffusion and clustering on Pd(111) *Science* **297** 1850–2
- [38] Stipe B C, Rezaei M A, Ho W, Gao S, Persson M and Lundqvist B I 1997 Single molecule dissociation by tunneling electrons *Phys. Rev. Lett.* **78** 4410–3
- [39] Zambelli T, Barth J V, Wintterlin J and Ertl G 1997 Complex pathways in dissociative adsorption of oxygen on platinum *Nature* **390** 495–7